

4. Vacancy formation in n-type silicon-doped GaAs

4.1 Introduction

Silicon is a widely used element for doping of gallium arsenide. Like other atoms of group IV, Si can occupy both the anion (arsenic) and cation (gallium) lattice sites exhibiting acceptor and donor properties, respectively. Usually the crystals grown from Ga solution by LPE (liquid phase epitaxy) have a p-type conductivity (Hicks and Greene 1960), whereas the material fabricated by both the Czochralski and Bridgman technique possesses a n-type conductivity. Due to the compensation effect, the concentration of conducting electrons (holes) is lower than the number of silicon dopants. The compensation reduces the doping efficiency and is a subject of great technological interest.

The compensation phenomenon in n-type heavily doped GaAs:Si was especially intensively investigated. In earlier studies, the electrical deactivation of silicon donors (Si_{Ga}^+) was attributed exclusively to silicon acceptors (Si_{As}^-), which were forming due to the amphoteric incorporation of Si atoms into the GaAs crystal lattice (Whelan et al. 1960). This mechanism is known as the “autocompensation”. However, in the late 80s, the analysis of infrared local vibrational mode (LVM) absorption showed that the autocompensation alone could not explain strong electrical deactivation of Si_{Ga} -donors in heavily Si-doped GaAs epitaxial layers (Maguire et al. 1987). Some years later, this was confirmed by near-edge and extended x-ray-absorption fine structure techniques (NEXAFS and EXAFS), see e.g. Refs. (Schuppler et al. 1993, 1995). It was established that only about half of the losses of the electrical activity could be explained by autocompensation and therefore some other compensating center had to be taken into account. A variety of the defects participating in the compensation was proposed: $\text{Si}_{\text{As}}\text{-Si}_{\text{Ga}}$ dimers (Schuppler et al. 1995), Si clusters (Muto et al. 1992) and $\text{Si}_{\text{Ga}}\text{V}_{\text{Ga}}$ (Maguire et al. 1987; McQuaid et al. 1992; Northrup and Zhang 1993; Newman 1994). The last of them, $\text{Si}_{\text{Ga}}\text{V}_{\text{Ga}}$, is of special interest, because the defect complexes of similar configuration were found to be responsible for the compensation in other n-type GaAs crystals, i.e. $\text{Te}_{\text{As}}\text{V}_{\text{Ga}}$ (Williams 1968; Hurlle 1977), $\text{Ge}_{\text{Ga}}\text{V}_{\text{Ga}}$ (Hurlle 1999) and $\text{S}_{\text{As}}\text{V}_{\text{Ga}}$ (Williams 1968; Gutkin et al. 1995) in Te-, Ge- and S-doped GaAs. It was reasonable to suggest that the formation of donor-gallium vacancy complexes is a characteristic reaction of a GaAs crystal on n-type doping.

Although the first observations of $\text{Si}_{\text{Ga}}\text{V}_{\text{Ga}}$ complex formation date back to the 80's, the strongest evidence of their existence have come from relatively recent scanning tunneling microscopy (STM) (Domke et al. 1996) and positron annihilation (PALS) (Laine et al. 1996, Gebauer et al. 1997) studies of highly Si-doped GaAs ($[\text{Si}] \approx 10^{19} \text{ cm}^{-3}$). The combination of these two methods has allowed to determine directly the defect microstructure (STM) and the absolute concentration (PALS). It was shown that the $\text{S}_{\text{Ga}}\text{V}_{\text{Ga}}$ concentration increased dramatically (up to 10^{19} cm^{-3}) vs Si content and that increase was related to strong compensation at high doping levels. Thereafter, some simplified compensation models were developed, in which two types of acceptors, Si_{As} and $\text{Si}_{\text{Ga}}\text{-V}_{\text{Ga}}$, were taken into account (Birkmann et al. 2002). Those models explain satisfactorily the electrical deactivation at high ($>10^{18} \text{ cm}^{-3}$) Si concentrations (see the solid line in Fig. 4.1), whereas the defects formed for lower doping levels are less investigated. Another drawback of those compensation models is the widely used assumption that the compensation degree depends solely on Si content. In other words, the concentration of acceptors responsible for compensation is supposed to be a function of $[\text{Si}]$ only. This may be accepted just as a rough approximation.

The aim of this chapter is to give an overview of defects studies in GaAs crystals doped with silicon, the concentration of which varies over a wide range from 10^{17} cm^{-3} up to 10^{19} cm^{-3} . Some already published results have been complemented with those obtained in this work. The chapter is organized as follows: in Section 4.2 the results of investigations of heavily doped GaAs:Si, in which the compensation due to $\text{Si}_{\text{Ga}}\text{-V}_{\text{Ga}}$ complex dominates, are presented. In Section 4.3, it is shown that the compensation degree in a GaAs:Si wafer may be influenced by local dislocation density distribution. In Section 4.4, the origin of the defect that gives rise to the 1250 nm (0.95 eV) luminescence peak is discussed. It is demonstrated that this defect contributes to the vacancy signal detected by PALS in crystals with the silicon concentration of $[\text{Si}] < 10^{18} \text{ cm}^{-3}$. The defect was not observed in previous studies of heavily doped GaAs:Si since high silicon concentration suppresses its formation.

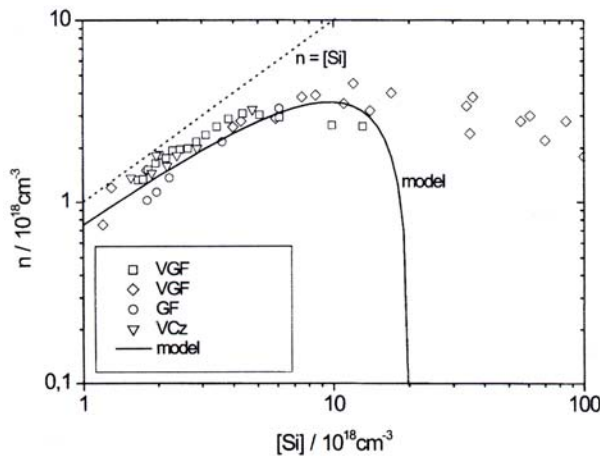


Fig. 4.1 Carrier concentration, n , versus the concentration of silicon dopants, $[\text{Si}]$, in GaAs:Si crystals grown with different techniques. The solid line represents a compensation model from Ref. (Birkmann et al. 2002)

4.2 Heavily silicon doped GaAs

Gallium arsenide doped with silicon in the range of $10^{18} - 10^{19} \text{ cm}^{-3}$ was extensively investigated by various experimental techniques including the positron annihilation. Therefore, the results presented in this section do not really extend the state of knowledge about point defect formation in this material. They were included into this chapter in order to give a complete picture of point defects in GaAs:Si. In addition, investigations of highly doped GaAs:Si represent a starting point for further studies of less doped material providing reference annihilation parameters for the identification of the well-investigated $\text{Si}_{\text{Ga}}\text{V}_{\text{Ga}}$ centers.

4.2.1 Experimental

The investigated samples were prepared using VGF boron-encapsulated crystals grown in the Crystal Growth Laboratory of the Department of Materials Science at the University of Erlangen. Their specifications are presented in Table 4.1. The Si and free charge carrier concentrations were determined by SSMS (Spark Source Mass Spectrometry, Dr. Wiedemann, Frankfurt University) and by Hall effect measurements (Dr. B. Birkmann, Erlangen University). The concentration of boron was in the same order of magnitude as that of silicon.

Table 4.1 Specifications of the heavily Si-doped GaAs VGF-grown crystals investigated in this work

Si concentration, cm^{-3}	Density of free charge carriers, cm^{-3}	Mobility, cm^2/Vs
1.61×10^{18}	1.40×10^{18}	1994
2.59×10^{18}	2.07×10^{18}	1724
3.55×10^{18}	3.05×10^{18}	1506
9.73×10^{18}	2.82×10^{18}	1085

The samples were investigated by positron lifetime and coincidence Doppler-broadening spectroscopy. The measurement procedure is described in Section 3.4.

4.2.2 Defect identification by means of positron annihilation

Average positron lifetime τ_{av} versus temperature obtained for GaAs doped with silicon at different doses is presented in Fig. 4.2. The temperature dependences of τ_{av} are similar for all samples indicating the same defects configuration. The magnitude of τ_{av} increases with temperature and reaches some value of saturation at $T > 300 \text{ K}$ that is distinctly higher than the bulk positron lifetime in GaAs, $\tau_{\text{b}} = 230 \text{ ps}$ (Gebauer et al. 2000). The increased average lifetime results from positron trapping into vacancy-like defects. The decomposition

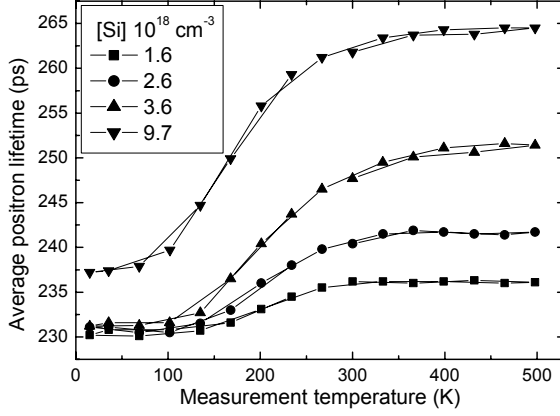


Fig. 4.2: Average positron lifetime as a function of measurement temperature in highly Si-doped VGF-grown GaAs. The concentrations of silicon dopants are indicated. The lines are to guide the eye.

of lifetime spectra by two components yielded the vacancy related lifetime $\tau_v = 262 \pm 5$ ps in all samples except the one with the highest Si content. For this sample, the vacancy concentration exceeded the PALS's sensitivity limit leading to the saturated positron trapping, i.e. the annihilation of all positrons took place in the vacancy-defect. As a result of the saturated trapping, all high temperature spectra had a single component τ_v equal τ_{av} . The lifetime of 262 ps is a typical value for a monovacancy in GaAs. The result gives a certain reason to believe the difference of the τ_{av} values over the range of saturation (see Fig. 4.2) is due to the change of the concentration of the defects having the same configuration.

At low temperatures, τ_{av} is close to τ_b indicating predominant trapping of positrons by non-open volume defects. Such defects are known as positron shallow traps and are commonly attributed to ionized acceptor-like ions, which are able to trap positrons into their negative potential (Saarinen et al. 1989). Since there is no open volume associated with the ions, the positron lifetime τ_{st} related to them is equal τ_b , $\tau_{st} = \tau_b = 230$ ps. Thus, the observed temperature behavior of τ_{av} can be thus explained by competitive positron trapping into two defect types – vacancies and shallow traps:

$$\tau_{av}(T) = (1 - \eta_{st}(T) - \eta_d(T))\tau_b + \eta_{st}(T)\tau_{st} + \eta_v(T)\tau_d, \quad (4.1)$$

where η_{st} and η_v are the fractions of positrons trapped by shallow trap and vacancy-like defects, respectively.

A similar temperature dependence of τ_{av} was observed by J. Gebauer et al. in other heavily Si-doped GaAs samples (Gebauer et al. 1997) investigated by PALS and STM spectroscopy. It was demonstrated rather conclusively that the two defects responsible for positron trapping were $\text{Si}_{\text{Ga}}\text{V}_{\text{Ga}}$ complexes and Si_{As} acceptors. For the vacancy complex, nearly the same positron lifetime ($\tau_v = 262 \pm 2$ ps) as in the samples studied in this work was found. The similar τ_v as well as the qualitative agreement between the τ_{av}

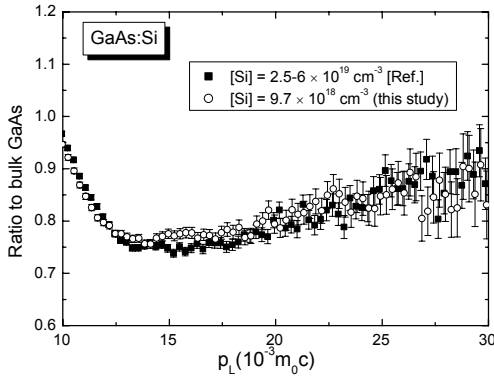


Fig. 4.3: High momentum part of Doppler broadening peak normalized to the data of bulk GaAs. (■) corresponds to GaAs:Si studied by positron annihilation and STM spectroscopy (Gebauer et al. 1997); (○) this study

temperature dependences allows to make the assumption concerning similarity of the microstructure of the defects observed.

In addition, the sample with the highest vacancy concentration was investigated by coincidence Doppler broadening spectroscopy (CDBS). The high momentum part of the annihilation Doppler peak normalized to the data obtained for GaAs reference is shown in Fig. 4.3. Solid squares correspond to the data taken from Ref. (Gebauer et al. 1999), which were obtained for the GaAs:Si sample investigated by STM in Ref. (Gebauer et al. 1997). The momentum distributions of the annihilation radiation in both samples are practically identical. This supports the assumption made above concerning the similar origin of the vacancy defect observed in this study and in the works done earlier (Gebauer et al. 1997). Two types of the point defects detected by positrons in heavily doped GaAs:Si were identified as $\text{Si}_{\text{Ga}}\text{V}_{\text{Ga}}$ complex and Si_{As} acceptor.

4.2.3 Model of the compensation mechanism

In this subsection, a simplified model of the compensation in GaAs:Si is discussed. The main goal of the model is to show that the formation of $\text{Si}_{\text{Ga}}\text{V}_{\text{Ga}}$ complexes can qualitatively explain the strong electrical deactivation of silicon donors (Table 4.1), which can not be understood in terms of autocompensation due to Si_{As} acceptors alone.

Two major assumptions have to be made. Firstly, three types of point defects are taken into account: Si_{Ga}^+ as the dominating donor and Si_{As}^- , $\text{Si}_{\text{Ga}}\text{V}_{\text{Ga}}^{2-}$ as two acceptors. The charge state of the vacancy complex is given as the sum of the charges states of Si_{Ga}^+ and $\text{V}_{\text{Ga}}^{3-}$ (Tan et al. 1993; You et al. 1993). Other Si-related defects (e.g., $\text{Si}_{\text{Ga}}\text{-Si}_{\text{As}}$ pairs and Si clusters) are known to become important for $[\text{Si}] \approx 3 \times 10^{18} \text{ cm}^{-3}$ (Suezawa et al. 1991) and can be neglected in the first approximation. Thus, the free carrier concentration can be evaluated as:

$$n = [\text{Si}_{\text{Ga}}] - [\text{Si}_{\text{As}}] - 2[\text{Si}_{\text{Ga}}\text{V}_{\text{Ga}}]. \quad (4.2)$$

The second assumption is that all silicon atoms are electrically active, i.e.:

$$[Si_{Ga}] = [Si] - [Si_{As}] - [Si_{Ga}V_{Ga}]. \quad (4.3)$$

The concentration of silicon atoms was determined by SIMS measurements (Table 4.1), $[Si_{Ga}V_{Ga}]$ and $[Si_{As}]$ could be extracted from the results of positron annihilation. The vacancy concentrations were calculated according to the one-defect two-component trapping model (Section 3.1.2) using the lifetime spectra measured at 500 K. At this temperature, positron trapping by shallow traps can be neglected due to the temperature detrapping of positron captured into the shallow negative potential of acceptor ions (Eq. 3.16). The decomposition of the spectra was performed at the fixed value of the vacancy-related lifetime, $\tau_{av} = 264$ ps. This lifetime corresponds to the maximum value of τ_{av} for positron saturated trapping (Fig. 4.2). The trapping coefficient μ_v was taken to be $1.7 \times 10^{15} \text{ s}^{-1}$ (Le Berre et al. 1995). After the vacancy concentrations were determined, the density of shallow traps could be obtained at 20 K using the three-state trapping model (Section 3.1.2). In this model, the positron annihilation at vacancy defects, negative ions and in the bulk is considered. According to the temperature dependence of the vacancy trapping coefficient (Puska and Nieminen 1994), the value of $\mu_v(20 \text{ K}) = 1.5 \times 10^{16} \text{ s}^{-1}$ was used. For the ions, $\mu_i(20 \text{ K}) = (5 \pm 2) \times 10^{16} \text{ s}^{-1}$ was taken (Saarinen et al. 1995; Gebauer et al. 1997). The values of concentration obtained by this procedure, $[Si_{Ga}V_{Ga}]$ and $[Si_{As}]$, are plotted in Fig. 4.4. For the highest level of doping, only the lower limit of vacancies concentration could be obtained due to the saturation observed for positron trapping.

As the number of acceptors has been determined, the concentration of free charged carriers may be easily calculated from Eqs. (4.2) and (4.3):

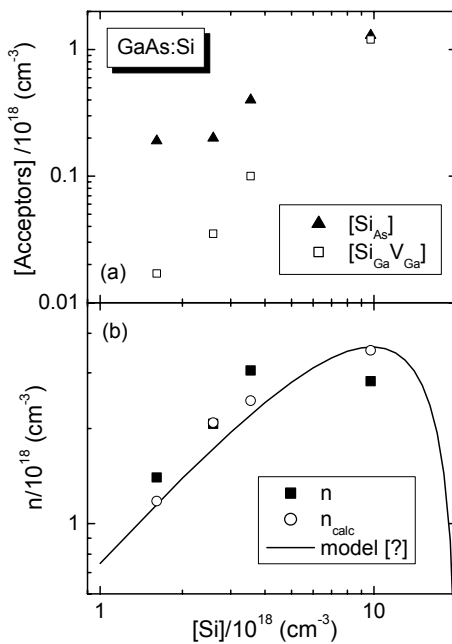


Fig. 4.4: (a) Concentration of acceptor-like defects ($Si_{Ga}V_{Ga}$, and Si_{As}) determined by positron annihilation lifetime spectroscopy as a function of Si concentration.

(b) Free electrons concentration directly measured (\blacksquare) and calculated (\circ) within compensation model using acceptors concentrations shown in (a).

$$n = [Si] - 2[Si_{As}] - 3[Si_{Ga}V_{Ga}]. \quad (4.4)$$

The calculated n_{calc} and directly measured n values of the carrier concentration are shown in Fig. 4.4 (b) as a function of $[Si]$. For the high values of $[Si]$, both n_{calc} and n demonstrate a deviation from the linear increase. This indicates the enhancement of the compensation degree at high doping levels due to the rapid increase of the concentration of the acceptor-like $Si_{Ga}V_{Ga}$ complexes [see Fig. 4.4 (a)]. However, n_{calc} is higher than n obtained for the sample having the highest concentration of silicon. The discrepancy observed can be explained as follows. In this sample, the concentration of $Si_{Ga}V_{Ga}$ complexes was underestimated due to the saturated positron trapping mentioned above; so the concentration of silicon acceptors was also underestimated, since Eq. (3.18) used for its calculation contains the quantity $[Si_{Ga}V_{Ga}]$. Therefore, the concentrations of acceptors used in (4.4) were lower than the real ones and n_{calc} hence higher than the real free electron density n . The solid line in Fig. 4.4(b) represents a compensation model developed in Ref. (Birkmann et al. 2002), which is based on a similar approach under the following assumption made on the acceptors concentrations:

$$[Si_{As}] = [Si]/11, \quad (4.5)$$

$$[Si_{Ga}V_{Ga}] = 2.3 \cdot 10^{16} \text{ cm}^{-3} \cdot ([Si]/10^{18} \text{ cm}^{-3})^{1.82}. \quad (4.6)$$

The dependence (4.5) was deduced from results of LVM measurements (Hannig et al. 1999); (4.6) is just a power-law fit to the published STM (Gebauer et al. 1997) and PALS (Laine et al. 1996; Gebauer et al. 1997) data on $Si_{Ga}V_{Ga}$. The results obtained by these approximations are in good agreement with the magnitudes of the $[Si_{As}]$ and $[Si_{Ga}V_{Ga}]$ concentrations under discussion in this thesis.

Summarizing the results, doping of GaAs by Si impurity results in the formation of acceptor-like $Si_{Ga}V_{Ga}$ complexes. The concentration of this complexes increases rapidly with the increasing doping level. The simplified compensation model based on direct measurements of the concentration $Si_{Ga}V_{Ga}$ by positron annihilation correctly describes the $[Si]$ - n -relationship for the range of concentrations $[Si] < 10^{19} \text{ cm}^{-3}$ (Fig. 4.1 and Fig. 4.4). At higher doping levels, the model is not valid due to the formation of other defects (such as, e.g. Si-pairs and Si-clusters), which were not taken into consideration in the model. Moreover, the vacancy concentrations in GaAs doped with Si at doses higher 10^{19} cm^{-3} exceed the sensitivity limit of positron annihilation and thus cannot be established.

4.3 Influence of dislocations on the lateral distribution of $Si_{Ga}V_{Ga}$ complexes in Si-doped VGF GaAs wafers

The compensation model of GaAs:Si described in the previous section allows us to outline the acceptors concentration as a function of silicon content only. This section dis-

cusses the influence of the dislocation density on the distribution of $\text{Si}_{\text{Ga}}\text{V}_{\text{Ga}}$ complexes. The interrelation between the concentration of $\text{Si}_{\text{Ga}}\text{V}_{\text{Ga}}$ defects and dislocation density was noted by Baeumler et al. in a recent photoluminescence study (Baeumler et al. 2002). They found a variation of a PL (photoluminescence) signal across a GaAs:Si wafer with non-homogeneous distribution of dislocations. The intensity of the 1100 nm peak attributed usually to $\text{Si}_{\text{Ga}}\text{V}_{\text{Ga}}$ complex anticorrelated with the concentration of dislocations. Since PL is a non-quantitative method, series of the samples cut out from the same wafer were studied in this work by means of positron annihilation. (Section 4.3.2). The results of more detailed investigations are presented in Section 4.3.3; in particular, it was shown that the dislocations may induce the variation of $\text{Si}_{\text{Ga}}\text{V}_{\text{Ga}}$ concentration resulting in the variation of compensation degree over GaAs:Si wafer.

4.3.1 Experimental details

Two wafers obtained from different VGF-grown GaAs:Si crystals were investigated. In the following, the wafers are referred as numbers #1 and 2.

Wafer #1 was investigated earlier by photoluminescence spectroscopy (PLS) and by laterally resolved photoluminescence topography (PLT) measurements (Baeumler et al. 2002). PLS and PLT were performed at 2 K using 514 nm Ar^+ laser illumination with 60 μm diameter spot size. The signal was dispersed with 1 m monochromator equipped with grating blazed at 2000 nm (band width 3 nm) and detected with the LN_2 cooled Ge detector.

PLT measurements on wafer #2 were performed at room temperature (RT) with 634 nm laser beam using Si-Detector sensitive over the range of 320 to 1100 nm wavelength. 2D-distribution of free charged carriers' concentration was determined by infrared absorption (IRA) and Hall-Effect measurements at RT. For the IRA, 1064 nm laser was used. The distribution of dislocation density was determined by EPD (etch-pit density) topography measurements.

The silicon content was determined by SIMS (wafer #1) or AtES (Atom emission spectroscopy, wafer #2) and amounted to $1.5 \times 10^{18} \text{ cm}^{-3}$ and $(1.3 \pm 0.1) \times 10^{18} \text{ cm}^{-3}$ in wafers #1 and #2, respectively.

For PALS investigations, several pieces with the size of 5×5 mm were prepared from each wafer. The exact positions of the samples taken from wafers #1 and #2 are indicated in Fig. 4.7 and Fig. 4.10, respectively. The measurement procedure is given in Section 3.4

4.3.2 Correlation between photoluminescence and positron annihilation investigations of silicon doped VGF GaAs

A typical PL spectrum of VGF GaAs:Si contains four luminescence band (Fig. 4.5, Table 4.2).

Table 4.2 - Assignment of photoluminescence lines in VGF GaAs:Si (Williams 1968; Tajima et al. 1994)

Label	Wavelength (nm)	Energy (eV)	Transitions from conduction band and shallow donors (Si_{Ga}) to valence band and shallow acceptors (Si_{As}^0 and B_{As}^0)
BN	832	1.49	
e, B_{As}^-	922	1.34	B_{As}^-
Si-Y	1100	1.13	$Si_{Ga}V_{Ga}$ acceptor level
X	1250	0.99	Undefined deep center, X

The luminescence intensities of these bands were found to be dependent on the position of the measurement on the wafer. The intensities of Si-Y and X bands increase from the wafer's center towards its edge whereas the intensities of BN and (e, B_{As}^-) bands were found to be higher at the center of the wafer (Fig. 4.5).

Full wafer topograms of wafer #1 shown in Fig. 4.6 present a more detailed pic-

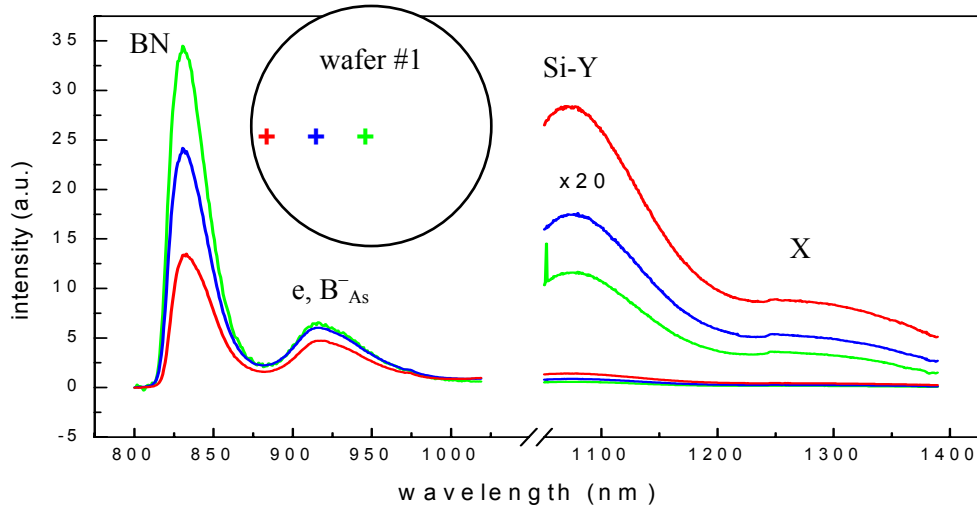


Fig. 4.5: Photoluminescence spectra measured in VGF GaAs:Si wafer #1. Curves of different colors correspond to different measurement positions on the wafer as indicated schematically by the colored crosses. Intensities of the bands with wavelengths higher 1050 nm are shown explicitly with 20 \times magnification. The spectra were not normalized. (From Ref. (Baeumler et al. 2002))

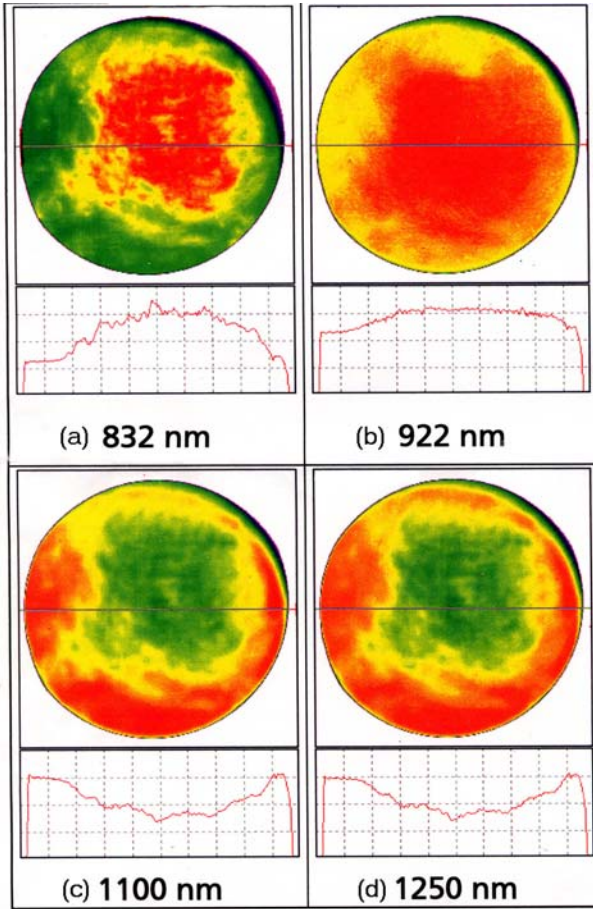


Fig. 4.5: Photoluminescence topograms of wafer #1 measured for the four luminescence lines occurring in GaAs:Si (see Fig. 4.5). (From Ref. (Baeumler et al. 2002)). The assignments of each PL-band are given in Table 4.2.

ture of the lateral intensity variation of each luminescence line. The variations were not connected with the distribution of silicon dopants across the wafer, since the latter was constant as determined by SIMS. In contrast, etching experiments revealed non-homogeneous distribution of local dislocation density. It was found that the intensity of the shallow (832 nm and 922 nm) transitions correlates whereas its value for the deep transitions (1100 nm and 1250 nm) anticorrelates with the EPD patterns. Such intensity variation can be explained either with the concentration variation of transition centers itself or by the presence of some non-homogeneously distributed non-radiative recombination center (NRRC). Thus, the dislocations can act as NRRCs in GaAs (Hoering 2001). On the other hand, dislocations are known to change the stoichiometry in the surrounding volume (Weyher et al. 1992). The area around the dislocations may contain less gallium vacancies and thus less $\text{Si}_{\text{Ga}}\text{V}_{\text{Ga}}$ resulting in a reduction of the 1100 nm photoluminescence peak. The problem can be resolved by direct measurement of the $\text{Si}_{\text{Ga}}\text{V}_{\text{Ga}}$ distribution by positron annihilation measurements.

For PALS investigation, the central part of the wafer #1 was cut into 15 sample pairs as shown in Fig. 4.7. Average positron lifetime τ_{av} is presented in Fig. 4.8 as a function of measurement temperature. The dashed line indicates the positron lifetime in the bulk GaAs, τ_{b} . The temperature behavior of τ_{av} is similar to the one observed in heavily

doped GaAs:Si investigated in the previous section. At high temperatures, τ_{av} is distinctly higher than τ_b due to positron trapping into vacancies. The decrease of τ_{av} towards low temperatures is evidence of the presence of positron shallow traps, i.e., as it is generally accepted, negatively charged ions. Silicon and boron acceptors are good candidates for these shallow trap defects. The decomposition of the lifetime spectra has revealed the presence of a vacancy-like defect with positron lifetime close to 260 ps. It is in good agreement with the value of 262 ps found for $\text{Si}_{\text{Ga}}\text{V}_{\text{Ga}}$ (Section 4.2). By using the analogy with the heavily doped GaAs:Si, the vacancy defect observed in wafer #1 was also identified as silicon donor-gallium vacancy complex; the shallow positron traps were attributed to silicon and boron acceptors.

At this point, it is worth to draw the reader's attention to the small hysteresis of τ_{av} , observed for the sample pairs 1-2 and 29-30 at high temperature region (Fig. 4.8). Obviously, some vacancy-like defects were annealed during the measurement at 500 K. This cannot be the $\text{Si}_{\text{Ga}}\text{V}_{\text{Ga}}$ complex, since $\text{Si}_{\text{Ga}}\text{V}_{\text{Ga}}$ was found to be thermally stable up to 500 K (see Section 4.2, Fig. 4.2). Since the decomposition of the lifetime spectra into more than two components (i.e. more than one defect) was impossible, the positron lifetime related to the annealed defects should be in the order of that one for the monovacancy. The average positron lifetime measured in other samples did not demonstrate such hysteresis behavior indicating the positron trapping into the one type of defect only. Possibly, the concentration of the second defect in those samples was under the sensitivity limit of positron annihilation. The PL topogram recorded at the 1250 nm PL line shows the maximum of the luminescence intensity at the edges and minimum in the middle of the wafer [Fig. 4.6 (d)]. Since sample pairs 1-2 and 29-30 correspond to the wafer edges (Fig. 4.7), it is reasonable to suggest that the unknown defect gives rise to the 1250 nm photoluminescence peak. The origin of this peak is currently unknown (X-defect in Table 4.2). A more detailed discussion on this question is given in Section 4.4. At this stage, it should be noted that the X-center is a vacancy-like defect and its concentration in most of

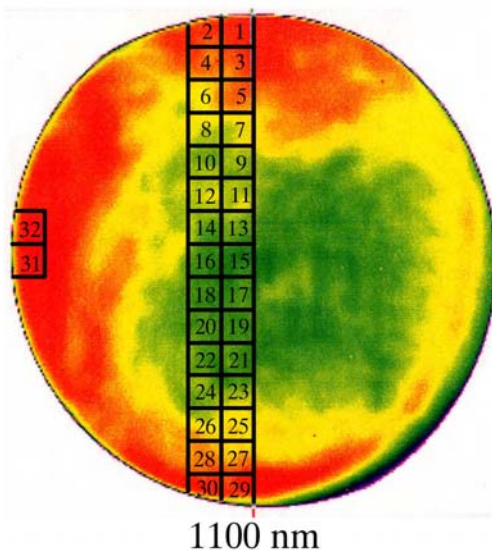


Fig. 4.7: Photoluminescence topogram image of wafer #1 recorded at the luminescence line of 1100 nm. Exact positions of the sample pairs taken for PALS measurements are indicated. The area of each single sample equaled 5×5 mm.

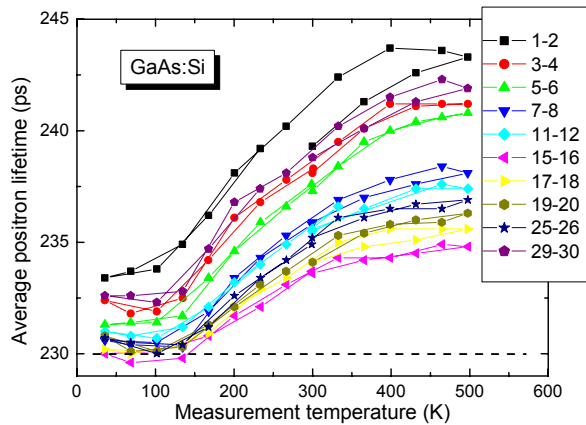


Fig. 4.8: Average positron lifetime vs temperature measured across the wafer #1. The sample numbers correspond to those shown in Fig. 4.7. The data points are connected by the lines in just the same consequence, the temperature measurements has been carried out (see Section 3.4).

the samples is too low to be detected by positrons.

The concentration of the $\text{Si}_{\text{Ga}}\text{V}_{\text{Ga}}$ complexes in each sample could be estimated from the lifetime data, as described in Section 4.2.3. For the samples 1-2 and 29-30, the vacancy concentration was determined after annealing of the X-defect. The obtained concentrations are plotted versus sample position in Fig. 4.9(a). As can be seen, the distribution of the vacancy complex is not constant, but reveals a minimum in the middle of the wafer replicating the intensity variation of the 1100 nm photoluminescence peak [fig. 4.9(b)]. The calculations of the concentrations of positron shallow trap performed by the three-state positron trapping model at 20 K yielded unrealistically large numbers (up to 10^{18} cm^{-3}) of the negative ions. Most probably, this is due to relatively low $\text{Si}_{\text{Ga}}\text{V}_{\text{Ga}}$ concentrations, at which the application of the three-state model is not possible.

Thus, we can conclude that the observed contrast of the 1100 nm (and, probably, of the 1250 nm) luminescence is caused by a non-uniform distribution of the deep centers, $\text{Si}_{\text{Ga}}\text{V}_{\text{Ga}}$ and the X-defect. The inverted contrast of the shallow transitions [Fig. 4.6 (a

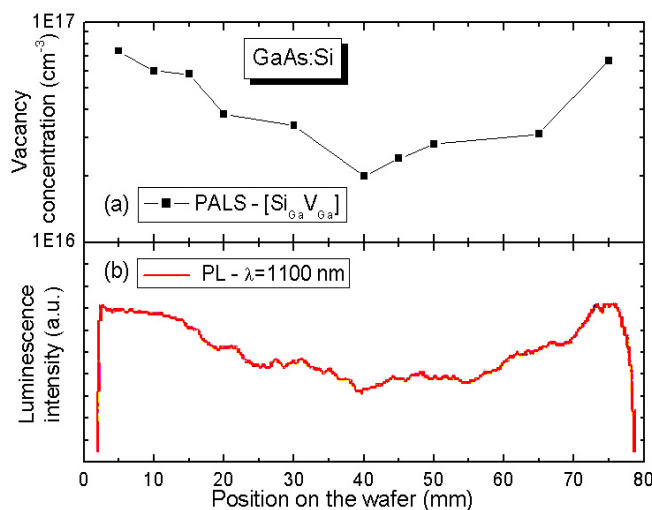


Fig. 4.6: (a) The distribution of $\text{Si}_{\text{Ga}}\text{V}_{\text{Ga}}$ complexes across the wafer #1, as determined by PALS

(b) intensity variation of the 1100 nm photoluminescence band, measured across wafer # 1 (From Ref. (Baeumler et al. 2002))

and b)] can be explained as a result of recombination competition, whence 832 nm and 922 nm intensity variations were caused indirectly by the variation of the deep centers concentration described above (Baeumler et al. 2002).

4.3.3 Lateral variation of the compensation degree in VGF GaAs:Si

This subsection continues the discussion on the influence of local dislocation density on the point defects formation in silicon doped VGF GaAs.

The combined photoluminescence and positron annihilation investigations (previous section) have rather clearly demonstrated the anticorrelation of the dislocation density and $\text{Si}_{\text{Ga}}\text{V}_{\text{Ga}}$ complexes distributions. However, these methods have not answered the question, whether the concentration of other point defects (Si_{Ga} and Si_{As}) and thus the compensation degree is also influenced by dislocations. This problem has been touched in this work by a systematic investigation of a VGF GaAs wafer (#2) with the help of SIMS, PALS, CDBS, IR absorption and electrical measurements (Bondarenko et al. to be published).

The EPD-topogram of wafers #2 (Fig. 4.10) revealed large variations of the local dislocation density in both wafers. The IR absorption measurements have shown a variation of the free electron concentration that replicated the EPD contrast (Fig. 4.11). In order to explain such correlation between n and EPD, two possible scenarios have been considered. Firstly, the increase of n may be merely due to non-homogeneous dopant (Si) distribution. The dislocation-rich regions thus have to have higher Si concentration than the rest of the wafer. The second scenario suggests lateral variation of the degree of compensation caused by dislocations-induced changes in concentration of electrically active point defects, i.e. Si_{Ga} , Si_{As} and $\text{Si}_{\text{Ga}}\text{V}_{\text{Ga}}$ (Section 4.2).

The first hypothesis has been examined by direct measurements of Si content; atom emission spectroscopy (AtES) has been applied. The analyzed samples were pre-

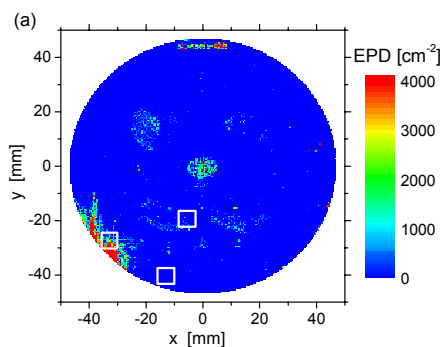


Fig. 4.7: Dislocation density distribution in wafer #2 obtained by EPD measurements. White squares denote the positions, from which the samples for PALS and AtES investigations were taken.

pared from wafers as shown by white squares in Fig. 4.10. Silicon concentration was

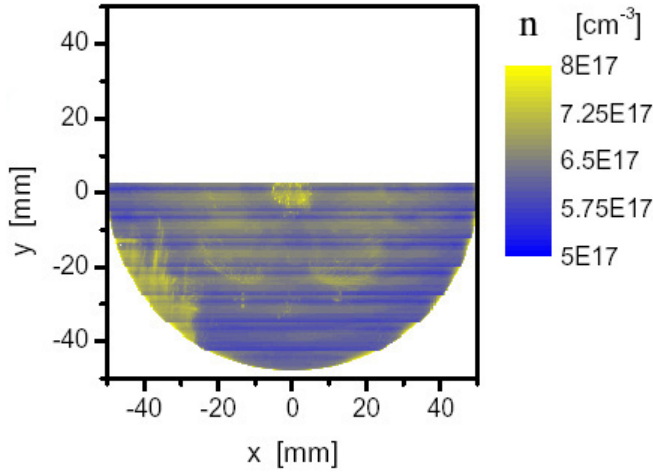


Fig. 4.8: Distribution of free charge carrier concentration in wafer #2 determined by IR absorption measurements.

found to be constant* in all samples and equaled $(1.3 \pm 0.1) \times 10^{18} \text{ cm}^{-3}$. Thus, the dislocation density does not influence the Si distribution and, therefore, the first scenario must be rejected. Consequently, the observed variation of n is due to different compensation ratios in dislocation-rich and dislocation-free regions. In order to give a quantitative interpretation of this discrepancy, one should identify the type of each defect participating in compensation as well as to evaluate their concentrations. As was shown in Section 4.2, for heavily-doped GaAs:Si these are single silicon donors, Si_{Ga} and two acceptors, Si_{As} and $\text{Si}_{\text{Ga}}\text{V}_{\text{Ga}}$.

Firstly, the type and concentration of the vacancy-complexes were determined by positron annihilation. Results of the lifetime measurements in the samples taken from wafer #2 are shown in Fig. 4.12. The vacancy-related defect, to be observed as the increase of τ_{av} over the bulk value ($\tau_{\text{b}} = 230 \text{ ps}$), has a positron lifetime τ_{v} close to 260 ps in all samples. This value is similar to $\tau_{\text{v}} = 262 \pm 5 \text{ ps}$ found for $\text{Si}_{\text{Ga}}\text{V}_{\text{Ga}}$ complexes (see Sections 4.2.2 and Ref. (Gebauer et al. 1997)). Also, the temperature dependence of τ_{av} is in good agreement with one observed in heavily doped GaAs:Si (Fig. 4.2). Therefore, the vacancies have also been identified as the Si_{Ga} -donor- V_{Ga} -vacancy complexes. The strong decrease of τ_{av} at low temperatures is due to the positron trapping by the Si_{As} acceptors acting as positron shallow traps with the positron lifetime close to τ_{b} .

The concentration of the vacancy complexes has been calculated according to the two-state one-defect trapping model using the lifetime data obtained at 300 K (Table 4.3). Similar to the results discussed in the previous section, the concentration of $\text{Si}_{\text{Ga}}\text{V}_{\text{Ga}}$ defects decreases with the increase of the dislocation density (Fig. 4.12). Bearing in mind the homogeneous distribution of the silicon dopants, the local reduction of $\text{Si}_{\text{Ga}}\text{V}_{\text{Ga}}$ concentration can explain the enhancement of free electron density observed in the dislocation-rich regions. However, this suggestion is valid only if the number of silicon donors

* Note: this observation is in agreement with constant silicon distribution found in wafer #1, Sec.4.3.2.

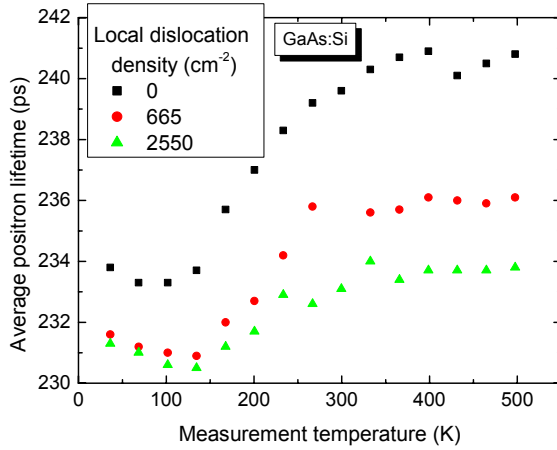


Fig. 4.12 Average positron lifetime vs temperature measured in three samples cut out from the regions of the wafer #2 having different concentration of dislocations. The sample positions are shown in **Fig. 4.10**. Dislocation densities are given in the legend.

and acceptors is constant across the wafer. It can be proved in the framework of the compensation model described in Section 4.2.3. Once the concentrations of free electrons, silicon and vacancy complexes are known, the concentrations of the silicon donors and acceptors can be calculated using the following linear system of equations:

$$\begin{aligned} [Si] &= [Si_{Ga}] + [Si_{As}] + [Si_{Ga}V_{Ga}] \\ n &= [Si_{Ga}] - [Si_{As}] - 2[Si_{Ga}V_{Ga}] \end{aligned} \quad (4.7)$$

The results of calculations and direct measurements are summarized in Table 4.3 and presented in Fig. 4.13. Si_{Ga} and Si_{As} concentrations are practically independent of dislocation density, whereas the formation of $Si_{Ga}V_{Ga}$ is found to be strongly suppressed by high concentration of dislocations.

Table 4.3 – Summary of directly measured and calculated data for VGF GaAs:Si samples with different dislocation density (wafer #2).

EPD (cm^{-2}) (measured)	n (cm^{-3}) (measured)	$[Si]$ (cm^{-3}) (measured)	$[Si_{Ga}V_{Ga}]$ (cm^{-3}) (measured)	$[Si_{As}]$ (cm^{-3}) (calculated)	$[Si_{Ga}]$ (cm^{-3}) (calculated)
0	8.77×10^{17}	1.3×10^{18}	5.7×10^{16}	1.26×10^{17}	1.12×10^{18}
665	1×10^{18}	1.3×10^{18}	3.1×10^{16}	1.0×10^{17}	1.17×10^{18}
2550	1.02×10^{18}	1.3×10^{18}	1.5×10^{16}	1.18×10^{17}	1.17×10^{18}

In summary, the correlation between local electrical properties and the dislocation density distribution was observed in silicon doped VGF GaAs wafers. It was shown that the correlation was not imposed by non-uniform distribution of silicon atoms, but related to the lateral variation of the degree of compensation. The latter is due to the suppression of formation of acceptor-like $Si_{Ga}V_{Ga}$ complexes by the high dislocation density. The concentration of $Si_{Ga}V_{Ga}$ complexes in dislocation-rich regions was reduced by 70% in

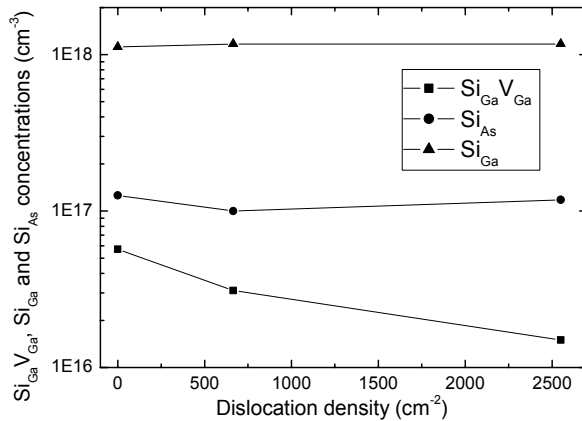


Fig. 4.13: Concentrations of donors (Si_{Ga}) and acceptors (Si_{As} , $Si_{Ga}V_{Ga}$) in silicon doped VGF GaAs as a function of the dislocation density.

comparison with the dislocations-free samples. In contrast to this, the incorporation of silicon as Si_{Ga} -donors or Si_{As} -acceptors was not affected much by dislocations.

4.4 Identification of the 0.95 eV luminescence band in VGF GaAs:Si

The discussion on point defects in silicon doped GaAs would be incomplete without a mention of the defect, which gives rise to 1250 nm (0.95 eV) luminescence band (Table 4.2). Though the occurrence of this band in n-type GaAs (e.g. in GaAs:Si, GaAs:Te or GaAs:S) has been known for a long time (Suezawa et al. 1994; Reshchikov et al. 1995; Toba et al. 1995), the attempts to attribute it to a certain defect are still controversial. A variety of defect types were proposed, e.g. acceptor-like ions (Toba et al. 1995), a $V_{As}Si_{Ga}V_{Ga}$ complex (Reshchikov et al. 1995) or $Si_{Ga}-Si_{As}$ pairs (Suezawa et al. 1994). However, neither of these defects was found to be consistent with the results of cathodoluminescence and positron annihilation investigations presented in this section. Instead, the set of possible candidates responsible for the illumination at 1250 nm is enriched by an additional defect type, the gallium vacancy.

4.4.1 Experimental

Two sets of samples have been investigated by the positron annihilation and cathodoluminescence spectroscopy. The first set corresponded to the one prepared from the VGF GaAs:Si wafer #1 (Section 4.3.1). Six samples of the second set have also been cut from a VGF GaAs:Si wafer. In order to avoid confusions, this wafer is referred in the following as wafer #3 keeping the general wafers numerating order of this chapter. In comparison to wafer #1 ($[Si] = 1.5 \times 10^{18} \text{ cm}^{-3}$, $n = 7.8 \times 10^{17} \text{ cm}^{-3}$), wafer #3 had lower concentration of

silicon dopants ($n = 1 \times 10^{17} \text{ cm}^{-3}$). However, exact Si-content in wafer #3 was not measured.

The cathodoluminescence spectroscopy was performed with a JSM 6400 scanning electron microscope (SEM) equipped with an Oxford monochromatic system. The range of temperatures from 20 K to 100 K was investigated. 20 keV electron beam was selected to excite the sample. A germanium (Ge) detector was used for collecting the corresponding CL spectra.

PALS measurements were performed according to the procedure described in section 3.4. The time resolution of the spectrometer was 240 ps.

Coincidence Doppler broadening spectroscopy (CDBS) was performed at 400 K and 200 K for the samples cut from wafer #1 and #3, respectively. The piece of undoped semi-insulating GaAs was taken as the material of reference and measured at room temperature. About 6×10^7 annihilation events were accumulated in each spectrum.

4.4.2 Cathodoluminescence spectroscopy

Fig. 4.14 represents the cathodoluminescence spectra measured in samples taken from wafers #1 and #4. Four luminescence bands denoted as A-D are assigned as given in Table 4.2. The origin of the defect responsible for the band D is unknown. For the sake of convenience, it will be further referred as X. The intensity of the band D is much higher in wafer #4 than in #1. In contrast, the band C related to $\text{Si}_{\text{Ga}}\text{V}_{\text{Ga}}$ complex is much

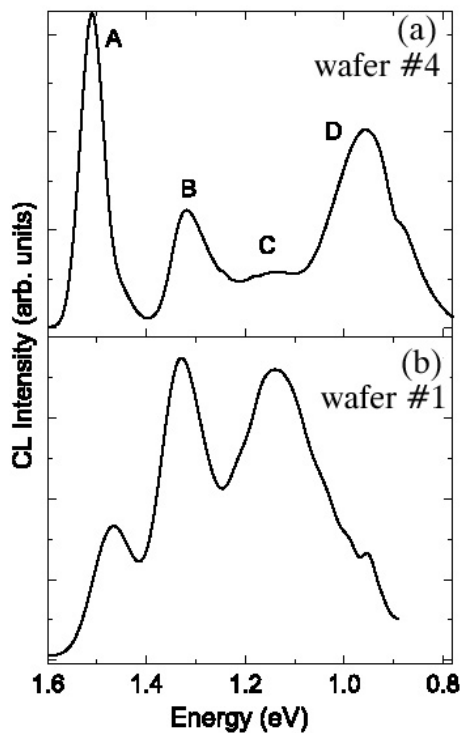


Fig. 4.14: Cathodoluminescence spectroscopy measurements on (a) wafer #4 and (b) wafer #1. Sample 2 was taken for investigation of wafer #1. CL spectroscopy was performed after PALS measurements. (From (Lei et al. 2003))

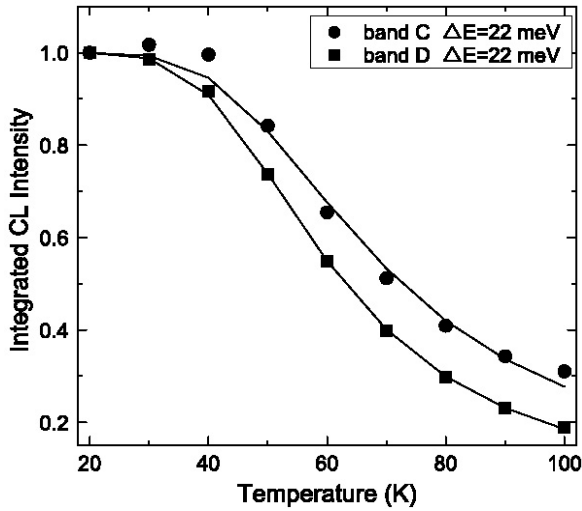


Fig. 4.15: Integral CL intensity of the luminescence bands C and D (see Fig. 4.14) as a function of temperature obtained in wafer #3. Intensity was normalized to the one at 20 K. Solid lines represent a fit according to Eq. 4.8

stronger in wafer #1. The intensity differences are due to the different concentrations of the corresponding defects (Yacobi and Holt 1990).

For the wafer #3, the luminescence bands C and D were measured in temperature interval from 20 K to 100 K. Their CL intensities vs temperature are shown in Fig. 4.15. Both intensities are characterized by the exponential decay:

$$I = I_0 [1 + C \cdot \exp(-\Delta E / k_B T)]^{-1}, \quad (4.8)$$

where C is a temperature-independent constant; k_B is Boltzmann constant and T is temperature; ΔE is an activation energy for thermal quenching processes introduced within the framework of configurational-coordinate (CC) model (for the model description see Ref. (Williams and Mackintosh 1968)). The model assumes that the light emission occurs by transition of the electron from the excited state associated with the donor atom to the ground state of the acceptor-like gallium vacancy. (Shionoya 1966). The ΔE is related to the position of the donor level in the band gap (Williams and Mackintosh 1968).

The value of ΔE can be determined by the analysis of the luminescence intensity as a function of temperature. A least-squares fitting according to Eq. (4.8) yielded the same $\Delta E = 22 \text{ meV}$ for both luminescence bands. This value is in good agreement with $\Delta E = 19 \pm 2 \text{ meV}$ found for $\text{Si}_{\text{Ga}}\text{V}_{\text{Ga}}$ complex in heavily silicon-doped GaAs (Sauncy et al. 1996). Similar ΔE implies the same position of the upper excited energy state for each recombination center, $\approx 20 \text{ meV}$ below the conduction band. The lower level of $\text{Si}_{\text{Ga}}\text{V}_{\text{Ga}}$ complex is known to be at about 0.3 eV above the valence band (Sauncy et al. 1996). Since the emission energy of the X defect (0.95 eV) is smaller than that for $\text{Si}_{\text{Ga}}\text{V}_{\text{Ga}}$ (1.2 eV), its ground state must be at $\approx 0.5 \text{ eV}$ above the valence band.

4.4.3 Defect identification by positron annihilation

The results of positron annihilation lifetime measurements are sufficiently different for wafers #1 and #3 (Fig. 4.8 and Fig. 4.16). The average positron lifetime τ_{av} increases continuously with increasing temperature in wafer #1, whereas the pronounced maximum at 200 K followed by a considerable decrease of τ_{av} is observed in wafer #4. Such large discrepancy of the τ_{av} temperature behavior points to a different nature of positron annihilation centers in both wafers. However, their vacancy-related lifetimes provided by one-defect spectra decomposition were found to be similar, $\tau_v = 260 \pm 5$ ps, the typical value for a monovacancy in GaAs. The vacancy-like defect in wafer #1 was previously identified as the $\text{Si}_{\text{Ga}}\text{V}_{\text{Ga}}$ complex (Section 4.2.2). The configuration of the vacancy-like defect in wafer #3 is currently unknown. It is reasonable to attribute the origin of this defect to the X-center that is responsible for the 0.95 eV luminescence band. Let us consider some aspects supporting this point.

First of all, the detailed investigation of the τ_{av} hysteresis observed in samples 1-2 and 29-30 of wafer #1 (Fig. 4.8) has led to the conclusion that some vacancy-like defects were annealed during the measurements at 400-500 K. As has already been noted in Section 4.3.2, this temperature is not high enough to cause the annealing of $\text{Si}_{\text{Ga}}\text{V}_{\text{Ga}}$ complexes. Hence, some other type of defects must be present. Since τ_{av} measured in other samples did not demonstrate such hysteresis, concentration of this defect must be higher at the wafers edge and too low to be detected with positrons in the middle of the wafer. Such lateral distribution is in agreement with the intensity variation of the 1250 nm (0.95 eV) photoluminescence line [Fig. 4.6 (d)]. As a check, one more pair of samples was cut from the edge of wafer #1 (samples 31-32, Fig. 4.7) and measured at temperatures from 300 K to 600 K. The expected hysteresis was indeed observed (Fig. 4.17). Thereafter the sample 2 (sample pair 1-2, wafer #1) was measured with cathodoluminescence at 75 K. As Fig. 4.14 (b) shows, the 0.95 eV CL peak disappeared. Thus, the assignment of the X-

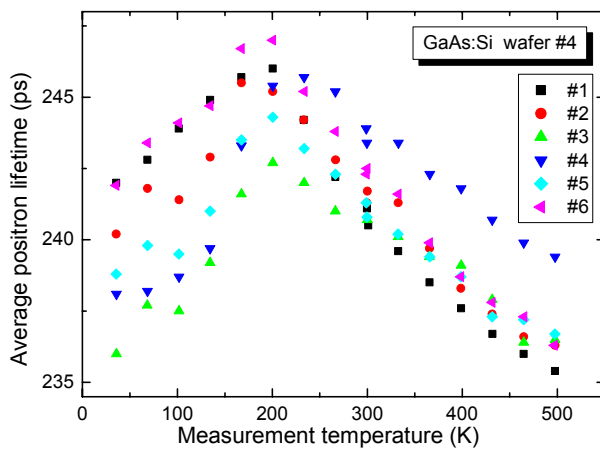


Fig. 4.9: Average positron lifetime as a function of temperature measured in the samples cut from silicon doped GaAs wafer #3.

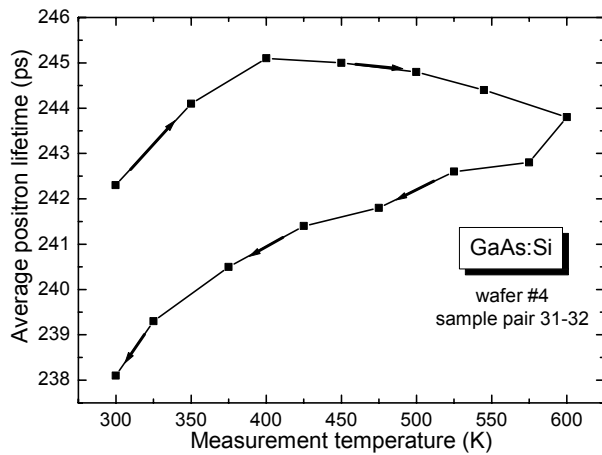


Fig. 4.10: The hysteresis of the average positron lifetime observed by temperature-dependent PALS-measurements performed on the sample pair 31-32 of GaAs:Si wafer #3. Samples position is shown in Fig. 4.7 The arrows indicate the order in which the measurements were performed.

defect responsible for 0.95 eV CL band to the unidentified vacancy-like defect observed with positron annihilation is justified.

As the next step, coincidence Doppler broadening (CDBS) measurements were performed in order to get additional information on electron momentum distribution at detected vacancies. Actually, the annihilation with core electrons, which are atom specific, is of interest here. In the case of a vacancy neighbored by some impurity or dopant atom (e.g., $\text{Te}_{\text{As}}\text{V}_{\text{Ga}}$ complex in GaAs:Te), the annihilation momentum distribution at vacancy-complex will differ from that of a single vacancy due to annihilation of positrons with core electrons of a foreign atom (Gebauer et al. 1999). Moreover, gallium and arsenic vacancies can be in principle differentiated with CDBS, since the core electron momentum distribution for As atoms surrounding V_{Ga} is different from that for Ga atoms, which are in the direct vicinity of V_{As} (Gebauer et al. 2001). Results of CDBS measurements revealed the same shape of annihilation momentum distribution for both wafers

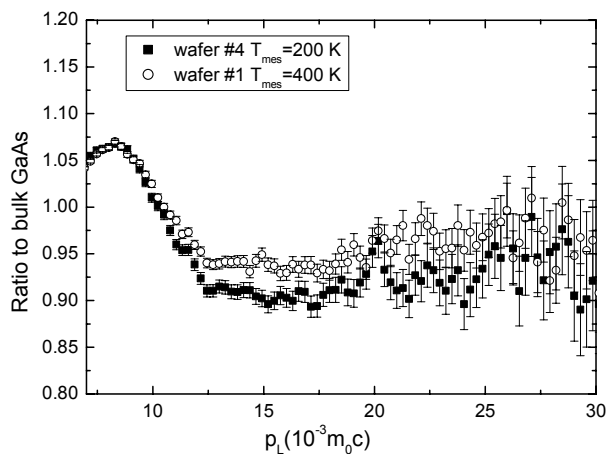


Fig. 4.18: Momentum distribution of the annihilation radiation obtained in the samples of wafers #1 and #3. The measurement temperature corresponded to the maximum trapping rate, i.e. to the longest τ_{av} (see Fig. 4.8 and Fig. 4.16).

(Fig. 4.18). This means the vacancy-like defects in wafer #1 ($\text{Si}_{\text{Ga}}\text{V}_{\text{Ga}}$) and in #3 (X-defect) belong to the same sublattice. Thus the X-defect must contain a gallium vacancy.

Summarizing the results of positron annihilation, photo- and cathodoluminescence spectroscopy, the following observations on the X-defect may be made: X represents a monovacancy-like defect that is mobile at 400-500 K. The electron momentum distribution at X is similar to that one measured for $\text{Si}_{\text{Ga}}\text{V}_{\text{Ga}}$ complex. Thus, X must be related to a gallium vacancy. However, τ_{av} demonstrates a quite different temperature dependence of positron trapping into X than into $\text{Si}_{\text{Ga}}\text{V}_{\text{Ga}}$ complex pointing to a different charge state of these defects. According to CL and PL measurements, the energy level of X lies approximately at 0.5 eV above the valence band; this is in good agreement with the ionization level provided by some calculations for triply negative V_{Ga} (Fig. 2.5). Formation of X is suppressed with increasing silicon concentration. Previously, X was always ascribed to some complex involving a donor-atom. However, in this work the same CL band was found in initially-undoped As-rich p-type GaAs (Section **Fehler! Verweisquelle konnte nicht gefunden werden.**, Fig. 6.7), which has low concentration of donor atoms. A monovacancy-like defect was found also in that material. Since the undoped GaAs was As-rich, the origin of the defect was attributed to the gallium vacancy. This is in agreement with the interpretation of the results discussed above. Thus, the X-defect relates to V_{Ga} and is not necessarily connected to a Si_{Ga} -donor. Taking into account that X was found also in p-type GaAs and bearing in mind it is mobile already at 500 K, it is reasonable to suggest that X does not belong to a donor- V_{Ga} complex but represents an isolated gallium vacancy.

4.5 Discussion: defects formation in VGF GaAs:Si

On the basis of the results of positron annihilation, photo- and cathodoluminescence spectroscopy the following mechanism of defect formation in silicon-doped GaAs is proposed. Since the growth takes place under As-rich conditions (Section 2), a large number of gallium vacancies V_{Ga} is present in the crystal. These vacancies can exist in different charge states: neutral, $-e$, $-2e$ or $-3e$. According to theoretical calculations of Tan et al. (Ref. (Tan et al. 1993)) triply-negatively-charged V_{Ga} dominate over the other charge states (Fig. 2.3). In an intrinsic, i.e. undoped, crystal the vacancy concentration decreases with decreasing temperature during cooling down the crystal. In the case of a doped crystal, the concentration of charged vacancies depends on the charge carrier concentration or on the position of the Fermi level, which is the so-called Fermi-level effect (Section 2.3). The equilibrium V_{Ga} concentration increases as n increases in n-type GaAs. Moreover, Tan et. al. showed that due to the Fermi-level effect the concentration of $\text{V}_{\text{Ga}}^{3-}$ is either independent of temperature or even shows a small negative temperature dependence. That is, as the temperature is lowered, the $[\text{V}_{\text{Ga}}^{3-}]$ is either unchanged or increases (Fig. 2.3).

Thus, Si doping increases the solubility of V_{Ga}^{3-} at the growth temperature. At high doping levels ($[\text{Si}] > 10^{18} \text{ cm}^{-3}$) gallium vacancies form $\text{Si}_{\text{Ga}}V_{\text{Ga}}$ acceptor complexes due to Coulomb attraction of Si_{Ga}^+ -donors and V_{Ga}^{3-} -acceptors. These complexes give rise to the 1100 nm luminescence band. At moderate level of doping, not all gallium vacancies are able to find a Si_{Ga} neighbor. It does not necessary mean that the vacancy concentration is higher than that of Si. Most probably, the density of Si donors is not high enough for a negative vacancy to feel the positive charge of a Si_{Ga} -donor. According to the Fermi-level effect, V_{Ga}^{3-} remains stable also after cooling down of the crystal. The monovacancies are seen as 1300 nm luminescence band in wafers #1 and #4. If the concentration of Si dopants is further decreased, the number of monovacancies will dominate over that of $\text{Si}_{\text{Ga}}V_{\text{Ga}}$ complexes. This results in a higher intensity of the 1300 nm luminescence band in comparison with the 1100 nm band in wafer #3.

The main argument against the interpretation given above consists in the commonly accepted fact that isolated Ga vacancies are not stable at temperatures above room temperature. Hautojärvi et al. observed annealing of monovacancy-type defects, which had been introduced by low-temperature electron irradiation, at 400 K. In the samples investigated in this study, vacancy-like defects have been found to be stable up to 500 K (the highest measurement temperature). However, the vacancies observed by Hautojärvi et al. had been created at low temperatures and hence were not in thermodynamic equilibrium. Therefore, there was a “thermodynamic driving force” tending to move the crystal into the equilibrium state by eliminating of excess vacancies. In contrast, the vacancies in the as-grown crystal studied here had been formed at high temperature and remained after the cooling down the crystal, because their presence is energetically favorable, as explained above.